Hydrol. Earth Syst. Sci., 21, 2463–2481, 2017
www.hydrol-earth-syst-sci.net/21/2463/2017/
doi:10.5194/hess-21-2463-2017

Hydrology and Earth System Sciences
Open Access
EGU

Regionalizing nonparametric models of precipitation amounts on different temporal scales

Tobias Mosthaf and András Bárdossy

Institute for Modeling Hydraulic and Environmental Systems, Universität Stuttgart, Stuttgart, Germany

Correspondence to: Tobias Mosthaf (tobias.mosthaf@iws.uni-stuttgart.de)

Received: 2 September 2016 – Discussion started: 17 October 2016
Revised: 29 March 2017 – Accepted: 9 April 2017 – Published: 10 May 2017

Abstract. Parametric distribution functions are commonly used to model precipitation amounts corresponding to different durations. The precipitation amounts themselves are crucial for stochastic rainfall generators and weather generators. Nonparametric kernel density estimates (KDEs) offer a more flexible way to model precipitation amounts. As already stated in their name, these models do not exhibit parameters that can be easily regionalized to run rainfall generators at ungauged locations as well as at gauged locations. To overcome this deficiency, we present a new interpolation scheme for nonparametric models and evaluate it for different temporal resolutions ranging from hourly to monthly. During the evaluation, the nonparametric methods are compared to commonly used parametric models like the two-parameter gamma and the mixed-exponential distribution. As water volume is considered to be an essential parameter for applications like flood modeling, a Lorenz-curve-based criterion is also introduced. To add value to the estimation of data at sub-daily resolutions, we incorporated the plentiful daily measurements in the interpolation scheme, and this idea was evaluated. The study region is the federal state of Baden-Württemberg in the southwest of Germany with more than 500 rain gauges. The validation results show that the newly proposed nonparametric interpolation scheme provides reasonable results and that the incorporation of daily values in the regionalization of sub-daily models is very beneficial.

1 Introduction

Rainfall time series of differing temporal resolutions are needed for various applications like water engineering design, flood modeling, risk assessments and ecosystem and hydrological impact studies (Wilks and Wilby, 1999; Burton et al., 2008). As many precipitation records are too short and contain erroneous measurements, stochastic precipitation models can be used to generate synthetic time series instead. Starting from single-site models (summarized in Wilks and Wilby, 1999) and multisite models for simultaneous time series at various sites (e.g., Wilks, 1998; Buishand and Brandsma, 2001; Bárdossy and Plate, 1992), models that allow for gridded simulations are finally developed (e.g., Wilks, 2009; Burton et al., 2008).

For modeling precipitation, one crucial variable is the precipitation amount, which follows a certain distribution. Distributions of the daily precipitation amounts are strongly right skewed, with many small values and few large values (Wilks and Wilby, 1999; Li et al., 2012; Chen and Brissette, 2014). This also holds true for different temporal resolutions with increasing skewness for higher temporal resolutions and vice versa. This means that rainfall intensity distributions depend on the temporal scale of the observed values. Applying single-site or multisite precipitation models at ungauged locations requires the regionalization of the precipitation amount distributions. This can be done in two different ways.

1. Interpolate the precipitation amounts from observation points for every time step to the target location(s) and set up a distribution with the interpolated values.

2. Fit a distribution function to the precipitation amounts separately for each gauge and interpolate the distribution functions to the target location(s).

The first approach seems more straightforward, but exhibits several deficiencies, such as the overestimation of the rainfall probability, the underestimation of the variance and the

underestimation of the maximum rainfall value. In the Supplement Sect. S1, an example demonstrates these problems. Due to the relative inefficiency of the first interpolation approach, the second is preferred.

In most stochastic rainfall models, the theoretical parametric distribution functions are fitted to the empirical values using, e.g., the exponential distribution or the two-parametric gamma distribution (Wilks and Wilby, 1999; Papalexiou and Koutsoyiannis, 2012). It is possible to either interpolate the parameters of the theoretical distribution or to interpolate the moments (e.g., the mean and standard deviation) of the rainfall intensities (Wilks, 2008; Haberlandt, 1998). Lall et al. (1996) introduced a more flexible nonparametric single-site rainfall model, for which they used nonparametric KDEs with a prior logarithmic transformation to model daily rainfall intensities. They addressed the problem of regionalization by using nonparametric estimates of distribution functions. However, a different interpolation scheme is required for nonparametric estimations, as they do not use any parameter that can be simply interpolated.

In the present work, we introduce a regionalization strategy for nonparametric distributions and compare it to the traditional regionalization of parametric distributions for varying temporal resolutions from hourly to monthly scales. The common procedure to interpolate parametric distribution functions is outlined as follows.

1. Fit a parametric distribution (e.g., a gamma or exponential distribution) at each sampling site to the empirical distribution function (EDF).

2. Interpolate the moment(s) or parameter(s) of the fitted parametric distribution.

3. Set up the theoretical cumulative distribution function (CDF) at every interpolation target with the interpolated moment(s) or parameter(s).

The newly proposed procedure for the nonparametric distribution functions is the following.

1. Fit a nonparametric distribution to log-transformed rainfall values using a Gaussian kernel.

2. Estimate the interpolation (kriging) weights with the precipitation values of a certain quantile.

3. Apply these weights to the values of certain discrete quantiles.

4. Linearly interpolate the remaining quantile values to receive a continuous CDF for all target locations.

In Arns et al. (2013), a similar approach is used to interpolate the quantile value differences of water levels for a bias correction between the empirical distributions of the observed and modeled values at the German North Sea coast. In contrast to their work, entire theoretical distribution functions are estimated in our work through interpolation. Goulard and Voltz (1993) introduced a curve kriging procedure to regionalize fitted functions, which was further developed by Giraldo et al. (2011). Based on their work, Menafoglio et al. (2013) developed a universal kriging approach for the nonstationary interpolation of functional data, which was applied in Menafoglio et al. (2016) for the simulation of soil particle distribution functions. As CDF curves are special functions that are monotonically non-decreasing between 0 and 1, the curve kriging procedure additionally needs to be constrained to these conditions. Our approach can deal with these conditions directly.

After describing the study region Baden-Württemberg in Sect. 2, the concept of precipitation amount models is introduced in Sect. 3. The data selection in Sect. 4 is followed by an investigation of the spatial dependence of the precipitation amount models in Sect. 5. The theory of precipitation amount models is addressed in Sect. 6, and the basis of the proposed interpolation procedure for nonparametric models is established in Sect. 7. The application of different regionalization procedures for precipitation amount models is explained in Sect. 8. The implementation of daily rainfall observations within the interpolation of sub-daily distribution functions is outlined in Sect. 9. The resulting performance of the different precipitation amount models at the point locations and their regionalization is depicted in Sect. 10.

2 Study region and data

The study region is the federal state of Baden-Württemberg, which is located in the southwest of Germany. The Black Forest mountain range, in the west, and the Swabian Alps, extending from southwest to northeast, exhibit the highest elevations in Baden-Württemberg. The rising of large-scale moist air masses across the mountainous regions causes higher rainfall amounts on the windward side and lower amounts on the leeward side. In the summer months, slopes with differing inclinations lead to a warming of the air that triggers convection currents, leading to a greater number of showers and thunderstorms over the mountainous regions. This shows a dependence of rainfall on elevation with seasonal differences. The rain-bearing westerly winds lead to high rainfall amounts in the Black Forest. The relatively lower altitude of the Swabian Alps results in lower rainfall amounts as they lie in the shadow of the Black Forest (Landesanstalt für Umwelt, Messungen und Naturschutz Baden-Württemberg , LUBW).

The years from 1997 to 2011 are chosen as the investigation period, as the German Meteorological Service (DWD) set up many new rain gauges in 1997. A relatively homogeneous data set is obtained by only choosing gauges with observation periods greater than or equal to 5 years, which also provide rainfall measurements for at least 80 % of the

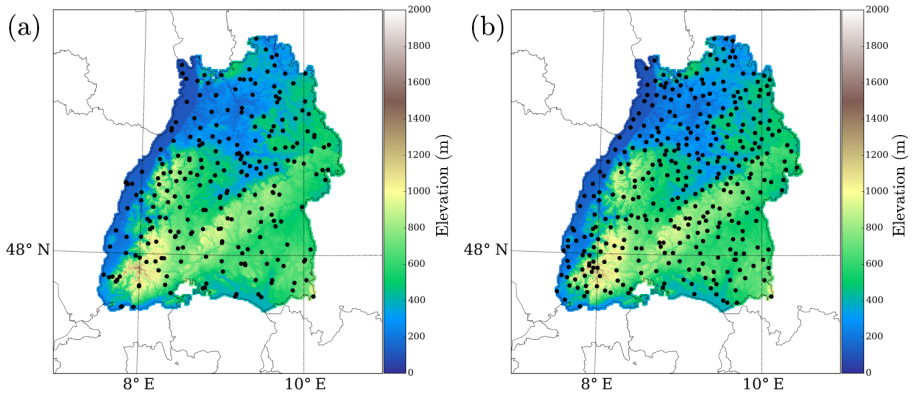

Figure 1. The locations of the high-resolution (hourly and 5 min; **a**) and daily rain gauges **(b)** in Baden-Württemberg.

time steps within their observation period. We had access to (i) 242 hourly and 5 min resolution and (ii) 347 daily gauges available in the study region, with 80 sites having both daily and high-resolution instruments. The observations are provided by the DWD and the Environmental Agency of Baden-Württemberg (LUBW). The high-resolution rain gauges are mostly equipped with tipping buckets and gravimetric measurement devices (Beck, 2013). Figure 1 shows the study region with the locations of the two sets of rain gauges.

3 Modeling precipitation amounts at point locations

Modeling precipitation amounts in our context means estimating the distribution functions. The usage of these distribution functions includes the implicit assumption of temporally independent and identically distributed (i.i.d.) variables. This assumption is generally accepted for daily rainfall as the autocorrelation of consecutive nonzero daily precipitation is relatively small and usually of less importance. For higher temporal resolutions, such as hourly, autocorrelation needs to be incorporated in the model (Wilks and Wilby, 1999). In practice, different methods exist to take such a correlation into account. One approach is to include autocorrelation prior to the sampling procedure by using conditional distributions. These conditions may be event statistics, like the duration of a rainfall event (e.g., Acreman, 1990), or varying statistical moments depending on the hour of the day (e.g., Katz and Parlange, 1995). Another approach is introducing autocorrelation after the sampling procedure. Bárdossy (1998) uses the empirical distributions of hourly rainfall intensities to sample values for which the random order is subsequently changed within a simulated annealing scheme to consider autocorrelation. In Bárdossy et al. (2000), the theoretical representations (CDFs) of the empirical distributions are used to allow for the regionalization of the distributions and enable simulations at ungauged locations. The non-exceedance probabilities of a CDF are referred to as *quantiles* in this work and their corresponding rainfall values are called *quantile values*.

4 Data selection

For the applications of rainfall estimates, like hydrological or hydraulic modeling, the correct representation of small rainfall values is not necessary as their contribution to decisively high discharge rates is rather small. Furthermore, tipping bucket gauges lead to wrong estimates, especially for low rainfall values (Habib et al., 2001). Relative estimation errors increase for decreasing rainfall rates (Nystuen et al., 1996; Ciach, 2003), and they only represent a small part of the total water volume, but the number of smaller rainfall values is rather high. To avoid the negative effect of this high number of inaccurate values and due to their minor importance for further applications, this study focuses on medium and high rainfall values.

Therefore, the quantile threshold (Q_{th}) for hourly (1 h) values is set to 0.95. This means that values smaller than the quantile value at $Q_{\text{th}} = 0.95$ are excluded. To investigate the total water volume represented by rainfall values above this quantile at point locations, the Lorenz curve (Lorenz, 1905) is used. We considered a water volume analysis for varying quantiles as important, to show that high quantiles not only represent the decisively higher rainfall intensities, but also a large proportion of the total water volume. Focusing on these quantiles during the model setup is likely to lead to a better model, as lower quantiles would disturb the model estimation due to measurement errors and the higher quantiles already represent a high percentage of the total water volume. The volume of the lower quantiles can then be modeled by simple and robust methods, as they do not require a very precise estimation due to their high inaccuracy and minor importance.

After arranging the n observations x_i in non-decreasing order, the Lorenz curve L_i can be calculated from a population (in our case, the rainfall values at a single gauge) with the following formula:

$$L(i) = \frac{\sum_{j=1}^{i} x_j}{\sum_{j=1}^{n} x_j}. \quad (1)$$

Table 1. The basic rainfall information of the study region for different aggregations (agg): P_0 is the probability of 0 mm rainfall, Q_{th} stands for the defined quantile thresholds or the threshold ranges and QV_{th} represents the corresponding quantile values (rainfall) for the defined Q_{th}.

Agg	P_0 (–)	Q_{th} (–)	QV_{th} (mm)
1 h	0.82–0.93	0.95	0.2–1.6
2 h	0.76–0.9	0.93	0.3–2.3
3 h	0.71–0.87	0.92	0.4–3.1
6 h	0.61–0.81	0.9	0.7–5.1
12 h	0.46–0.72	0.86	1.2–7.7
1 d	0.38–0.6	0.72	1.0–6.4
5 d	0.1–0.22	0.29	1.0–7.2
m	0.0–0.02	0.0–0.02	0

The hourly threshold quantile values (QV_{th}) range between 0.2 and 1.6 mm for $Q_{th} = 0.95$ depending on the location of the gauge (see Table 1). The Lorenz curve in Fig. 2a shows that the hourly values above $Q_{th} = 0.95$ represent between 70 and 95 % of the total water volume (100 % minus the cumulative share of the water volume).

Based on the hourly values (1 h) of the high-resolution data set, the aggregated rainfall values of different temporal resolutions are obtained: 2-hourly (2 h), 3-hourly (3 h), 6-hourly (6 h) and 12-hourly (12 h). Through the aggregation of the daily values (1 d) in the daily data set, 5-daily (5 d) and monthly (m) values are obtained. In order to exclude small values and still consider the values producing a high percentage of the water volume, the Q_{th} for the sub-daily resolutions are defined with the mean Lorenz curves in Fig. 2b. The mean hourly Lorenz curve yields 0.15 as the cumulative share of the water volume for $Q_{th} = 0.95$ (85 % of the total water volume is represented by larger values), which is also defined as the target share for the remaining sub-daily resolutions. This target share of 0.15 results in the following values of Q_{th} for the sub-daily resolutions: 0.93, 0.92, 0.9 and 0.86 (see Table 1). For aggregations greater than or equal to 1 day, the number of values is rather small and their estimation errors are lower due to an increasing accumulation time (Ciach, 2003; McMillan et al., 2012). Nevertheless, only the values above the highest quantile of 1 mm in the study region are used for the daily (1 d) and 5-daily (5 d) resolution (see Table 1), as the smaller values may still exhibit measurement errors.

For the estimation of the basic statistics in Table 1 and for the following calculations, the rain values of the investigated aggregations smaller than 0.1 mm are set to 0 mm. The reason is to achieve the homogenization of the data sets for different years and gauges, as the discretization ranges from 0.01 to 0.1 mm depending on the gauge.

5 Probability distributions of precipitation amounts in a spatial context

This section focuses on the spatial dependence of the precipitation amount distributions, as the applied interpolation technique of ordinary kriging (OK) is based on the assumption that the variable of interest (the CDF) is more likely to be dissimilar with increasing distances. For the purpose of describing the development of the distribution functions in space, the test statistic T of the two-sample Cramér–von Mises criterion is used (Anderson, 1962). It evaluates the similarity of two CDFs, in our case the similarity of the CDFs from the observations at two different point locations. The test statistic T is defined according to Anderson (1962) as

$$T = \frac{U}{NM(N+M)} - \frac{4MN-1}{6(M+N)}, \tag{2}$$

where

$$U = N \cdot \sum_{i=1}^{N} (r_i - i)^2 + M \cdot \sum_{j=1}^{M} (s_j - j)^2, \tag{3}$$

with N as the number of observations in the first sample and M as number of observations in the second sample. Both observations are joined together in one pooled data set, and the ranks are determined in ascending order of all observations in the pooled data set. The r_i values are the ranks of the N observations for the first sample in the pooled data set and s_j are the sorted ranks of the M observations for the second sample in the pooled data set. T can be interpreted as the mean difference in the CDF values (quantiles) of the observed rainfall intensities between the two data sets. So, if T increases for increasing distances, the CDFs are less similar for increasing distances.

For the calculations of T, only the rainfall values above the different Q_{th} (see Table 1) are used. The graphs in Fig. 3 show a decreasing similarity in the distribution functions with increasing distances over all temporal resolutions, as the values of T increase with increasing distances. Note that the average T values of the hourly (1 h) data in Fig. 3a are shown as the highest dashed line in Fig. 3b. The continuity of the whole distribution changes in space, and not only the continuity of the values in a single quantile. This shows the applicability of interpolation techniques like OK.

6 Precipitation amount models

In the following subsections, nonparametric and parametric models for precipitation amounts at single sites are introduced. Before estimating the nonparametric or parametric distributions at each observation gauge, the observations smaller than QV_{th} are censored from the sample of each gauge and QV_{th} is subtracted from the values above them to fit to the support of the theoretical distribution functions

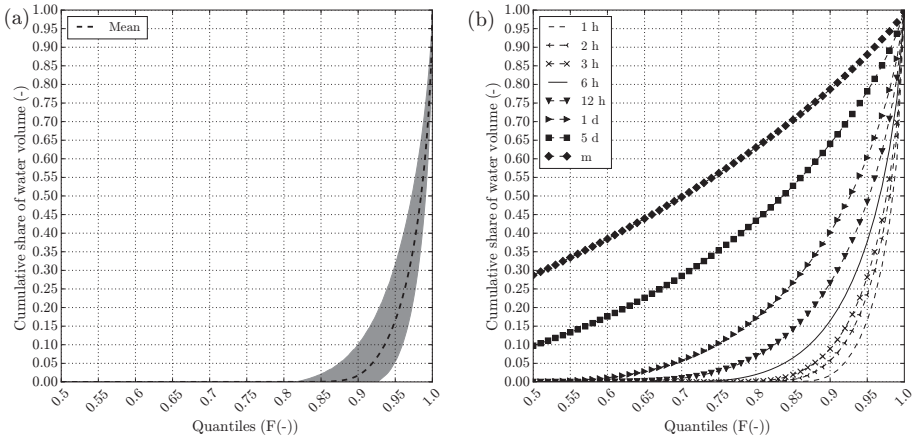

Figure 2. The **(a)** range of the Lorenz curves and the mean Lorenz curve for the hourly rainfall values of all the rainfall gauges inside the study region. The **(b)** mean Lorenz curves for different temporal resolutions.

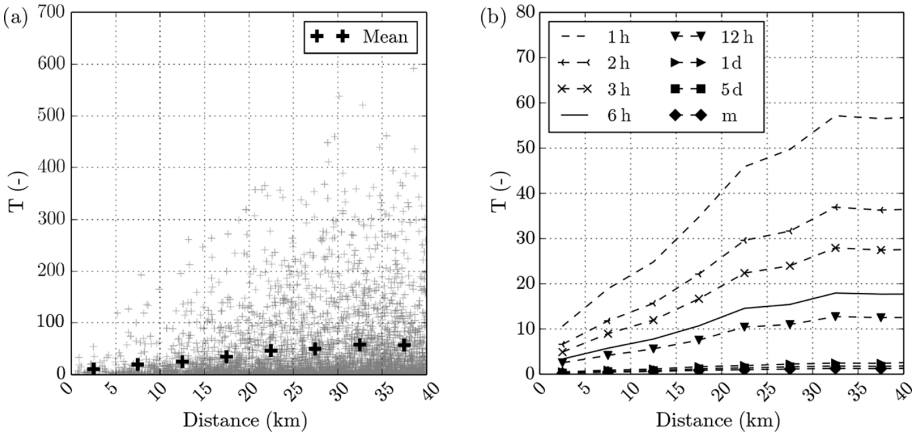

Figure 3. The T statistic over distance: **(a)** the results for the hourly distribution functions of all gauge pairs (the gray crosses) and their mean calculated for 5 km classes. **(b)** The mean values of the T statistic for different temporal resolutions (for more detail on the temporal resolutions of 1 d, 5 d and m, see Fig. S2).

$[0, \infty)$. QV_{th} varies from gauge to gauge for different temporal resolutions (see Table 1). After estimating the theoretical CDFs, the quantiles F are scaled with Q_{th}

$$F_{sc} = F \cdot (1 - Q_{th}) + Q_{th}, \tag{4}$$

and QV_{th} is added to the quantile values. Only the monthly resolution is excluded from the whole scaling procedure, as all monthly rainfall values are used.

6.1 Nonparametric models

The nonparametric KDEs for the precipitation amount distributions were previously used and are described for the daily precipitation amounts in Rajagopalan et al. (1997) and Peel and Wilson (2008). Using this nonparametric method means that no theoretical distribution needs to be preassigned; only a kernel and its bandwidth need to be chosen. That is why they are assumed to be more flexible. A kernel in this context is a function which is centered over each observation value and is itself a probability density function with a variance controlled by its bandwidth (Bowman and Azzalini, 1997). The probability density function (PDF) or KDE $f(x)$ of every data set is then constructed through a linear superposition of these kernels (Peel and Wilson, 2008), where n is the number of observed values, K is the kernel function, h is the bandwidth of the kernel, x are discrete kernel supporting points and x_i are observed rainfall values:

$$f(x) = \frac{1}{n} \sum_{i=1}^{n} K(x - x_i; h). \tag{5}$$

The estimation of $f(x)$ is performed with an R (R Core Team, 2015) implementation of Wand (2015). However, since our nonparametric interpolation scheme is based on CDFs and not on PDFs, the CDF is needed. In order to obtain a CDF from the KDEs, an integration is required, which is done numerically with the composite trapezoidal rule (e.g.,

Atkinson, 1989). For numerical reasons, quantiles slightly greater than 1 are sometimes obtained, which are simply set to 1 so that they remain in the correct range.

To model the right-skewed precipitation amounts with their bounded support on $[0, \infty)$, either an asymmetric kernel like the Gamma kernel (Chen, 2000) or a symmetric kernel with a prior logarithmic transformation of the values (Rajagopalan et al., 1997) can be used to avoid boundary bias. A boundary bias occurs when kernels with infinite support are used for data with bounded support, as this would lead to a leakage of probability mass (Rajagopalan et al., 1997).

In this work, the symmetric Gaussian kernel with a prior transformation of data to logarithms is chosen, as this is an implicit adaptive kernel method with increasing bandwidths for increasing values and therefore alleviates the need to choose variable bandwidths with skewed data (Lall et al., 1996; Charpentier and Flachaire, 2014). The Gaussian kernel is chosen as it is straightforward and its application is facilitated through several software implementations (Sheather, 2004). The Gaussian kernel $K(t)$ is described in Eq. (6):

$$K(t) = \frac{1}{h\sqrt{2\pi}} \cdot \exp\left(\frac{-t^2}{2h^2}\right). \tag{6}$$

If the density of the logarithmically transformed observed values $y = \log(x)$ is f_Y and a Gaussian kernel is used for this density estimation, the density estimation f_X of the original values x according to Charpentier and Flachaire (2014) is

$$f_X(x) = f_Y(\log(x))\frac{1}{x}. \tag{7}$$

Finally, the bandwidth h needs to be chosen, which is commonly indicated as the key step for KDEs (e.g., Bowman, 1984; Harrold et al., 2003; Sheather, 2004; Charpentier and Flachaire, 2014) as a poor bandwidth selection may result in a peakedness or an over-smoothing of the density estimation. Due to this great importance of the bandwidth selection, the performances of different selection methods are investigated.

1. The simplest and most widely used selection method is Silverman's rule of thumb (Silverman, 1986), which is defined as

$$h_{\text{opt, SRT}} = 0.9 \cdot \min\left(s; \frac{q_3 - q_1}{1.349}\right) n^{-1/5} \tag{8}$$

   to obtain the optimal kernel bandwidth $h_{\text{opt, SRT}}$ with n sample values, where s is the standard deviation and $q_3 - q_1$ is the interquartile range. Silverman's rule of thumb (SRT) is deduced by minimizing an approximation of the mean integrated squared error between the estimated and the true densities, where the Gaussian distribution is referred to as the true distribution (Charpentier and Flachaire, 2014).

2. The second method is a plug-in approach developed by Sheather and Jones (1991), which is widely recommended due to its good performance (Jones et al., 1996; Rajagopalan et al., 1997; Sheather, 2004). Instead of using a Gaussian reference distribution, it uses a prior nonparametric estimate in the approximation of the mean integrated square error and therefore requires a numerical calculation (Charpentier and Flachaire, 2014) to find the optimal bandwidth $h_{\text{opt, SJ}}$. This is performed with the R implementation of Wand (2015) within this work.

Instead of minimizing the mean integrated squared error, Bowman (1984) recommended minimizing the integrated squared error through a least squares cross-validation (LSCV), which is applied using the R package of Duong (2015). Another common cross-validation method is the maximum likelihood cross-validation (MLCV). Cross-validation methods tend to produce small bandwidths and therefore tend to produce a peakedness in the density (Rajagopalan et al., 1997; Sheather, 2004; Peel and Wilson, 2008), which we also observed in our applications. Due to this deficiency, neither cross-validation method is considered in what follows.

6.2 Parametric models

Within the parametric procedure, five different parametric distributions are used to model the precipitation amounts of all aggregations in this study. The most commonly used models are the exponential distribution and the two-parameter gamma distribution (Wilks and Wilby, 1999). The mixed-exponential distribution was recommended in Wilks and Wilby (1999) and was first used for daily precipitation amounts by Woolhiser and Pegram (1979). Another common and efficient distribution to model precipitation amounts, especially with daily temporal resolution, is the generalized Pareto distribution (Chen and Brissette, 2014; Li et al., 2012). In addition to these models, the Weibull distribution is used, which showed good performance for modeling monthly precipitation amounts in Baden-Württemberg (Beck, 2013). The CDF $F(x)$ and the PDF $f(x)$ of each parametric distribution used here are listed in the following.

1. For the exponential distribution with the parameter λ, these functions are

$$f(x;\lambda) = \lambda e^{-\lambda x}, \tag{9}$$

$$F(x;\lambda) = 1 - e^{-\lambda x}. \tag{10}$$

2. For the two-parameter gamma distribution, they are

$$f(x;\theta,k) = \frac{x^{k-1}e^{-\frac{x}{\theta}}}{\Gamma(k)\theta^k}, \tag{11}$$

$$F(x;\theta,k) = \frac{\gamma\left(k, \frac{x}{\theta}\right)}{\Gamma(k)}, \tag{12}$$

   where Γ is the gamma function and γ is the incomplete gamma function.

3. For the two-parameter Weibull distribution, $F(x)$ and $f(x)$ are

$$f(x;\lambda,k) = \frac{k}{\lambda}\left(\frac{x}{\lambda}\right)^{(k-1)} e^{-(x/\lambda)^k}, \quad (13)$$

$$F(x;\lambda,k) = 1 - e^{-(x/\lambda)^k}. \quad (14)$$

4. The mixed-exponential distribution exhibits the following functions:

$$f(x;\lambda_1,\lambda_2,\alpha) = \alpha\lambda_1 e^{-\lambda_1 x} + (1-\alpha)\lambda_2 e^{-\lambda_2 x}, \quad (15)$$

$$F(x;\lambda_1,\lambda_2,\alpha) = 1 - \alpha e^{-\lambda_1 x} - (1-\alpha)e^{-\lambda_2 x}. \quad (16)$$

5. The generalized Pareto distribution exhibits the following PDF

$$\begin{aligned} f(x;k,\alpha) &= \alpha^{-1}(1+kx/\alpha)^{-1-\frac{1}{k}}, \quad k \neq 0 \\ &= \alpha^{-1}e^{-x/\alpha}, \quad k = 0 \end{aligned} \quad (17)$$

and CDF

$$\begin{aligned} F(x;k,\alpha) &= 1-(1+kx/\alpha)^{-1/k}, \quad k \neq 0 \\ &= 1-e^{-x/\alpha}, \quad k = 0. \end{aligned} \quad (18)$$

The parametric distributions with more than two parameters are not considered, as this would complicate the regionalization of the distributions due to the dependencies among the parameters. For the three-parameter mixed-exponential distribution, the parameter α is fixed for the whole study region (Wilks, 2008), transforming it into a two-parameter distribution.

In order to estimate the optimal parameter sets of the presented parametric distributions for each rainfall gauge and temporal resolution, the method of moments (MOM) and the maximum likelihood method (MLM) using a numerical maximization via a simplex algorithm are applied. The MLM is applied to all mentioned parametric distributions. In the special case of the mixed-exponential distribution, the parameter α is varied between 0.01 and 0.5 within the parameter estimation. For each value of α, the sum of the log-transformed likelihoods is calculated over all gauges with varying values of the remaining parameters, while the maximum sum defines the parameter set. To apply MOM, the mean $\overline{x}$ and standard deviation s_x of the sample values need to be calculated for the gamma and generalized Pareto (Hosking and Wallis, 1987) distribution. In order to use MOM for the Weibull distribution, the method described in Cohen (1965) is applied. For the estimation of the mixed-exponential distribution parameters, MOM is not applied due to its shortcomings as described in Rider (1961). MOM is also not applied to the one-parameter exponential distribution, as it would yield the same results as those from the MLM.

7 Nonparametric distributions in a spatial context

In order to establish the basis of the proposed regionalization procedure for nonparametric models and to get a more detailed idea of the spatial relationship of the distribution functions, the EDFs of the hourly and monthly rainfall intensities from the gauge at Stuttgart/Schnarrenberg and its five closest gauges are plotted in Fig. 4. It is therefore not of importance which EDF belongs to which gauge, but rather the relationship that the EDFs have with each other. The two graphs in Fig. 4 show that the order of the EDFs stays quite persistent over different quantiles for both aggregations, as the EDFs do not cross each other very often. In other words, if one gauge exhibits the highest rainfall values for a certain quantile, it also exhibits the highest rainfall values for the other quantiles and vice versa. The red and purple EDFs on the left graph illustrate this quite nicely.

A more global look at the spatial relation between different EDFs can be obtained with the Spearman's rank correlation ρ_{xy} of the quantile values of all gauges for different quantile pairs. As we want to investigate the persistence of EDFs for the whole study region, we are only interested in the ranks, or rather the order, of the different quantile values for differing quantiles, which can be identified by calculating ρ_{xy}. In our application the two input data sets for calculating ρ_{xy} represent the quantile values of two different pairs of quantiles over all gauges in the study region. These pairwise rank correlations of the quantile values of all gauge pairs are calculated starting from Q_{th} until 1 in 0.001 steps for sub-daily aggregations and in 0.005 steps for aggregations greater than or equal to 1 day. This procedure is repeated until the rank correlation of every quantile with every other quantile is obtained. Finally the mean values of the rank correlation belonging to each quantile are calculated (see the dotted gray lines in Fig. 5). The highest mean rank correlation is indicated with a red cross in this figure, which also defines the control quantile (Q_{c}) with the highest mean rank correlation. The rank correlations of Q_{c} with the remaining quantiles lead to the dashed lines in Fig. 5.

Figure 5 demonstrates that most of the rank correlations are greater than 0.85, indicating a persistence of quantile values over a large interval of quantiles as well as over the whole study region for hourly through monthly data. Lower correlations can be observed for the highest and lowest quantiles, which indicates nonpersistent behavior for these quantiles. This behavior is similar for all temporal resolutions. Therefore, the quantile values of Q_{c} can be used to set up the interpolation weights. Applying these weights to the remaining quantiles from Q_{th} until 1 should lead to good regionalization results for nonparametric CDFs.

In Table 2, the control quantiles Q_{c} with the highest mean correlations are summarized for all temporal resolutions. As the precipitation mechanisms are different in summer and winter in Baden-Württemberg, the rainfall data sets are also analyzed separately for summer (from May to August) and

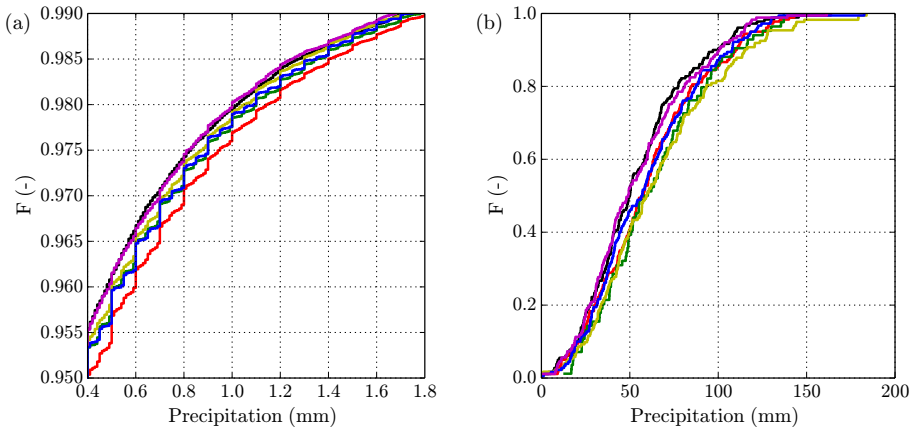

Figure 4. The EDFs of the hourly **(a)** and monthly **(b)** precipitation amounts for the gauge at Stuttgart/Schnarrenberg and its five closest gauges for a quantile interval. This shows that the order of the EDFs is quite persistent over a wide quantile range for low and high resolutions. Note: As the daily and hourly data sets are not the same, the colors in the two graphs do not correspond to the same gauges.

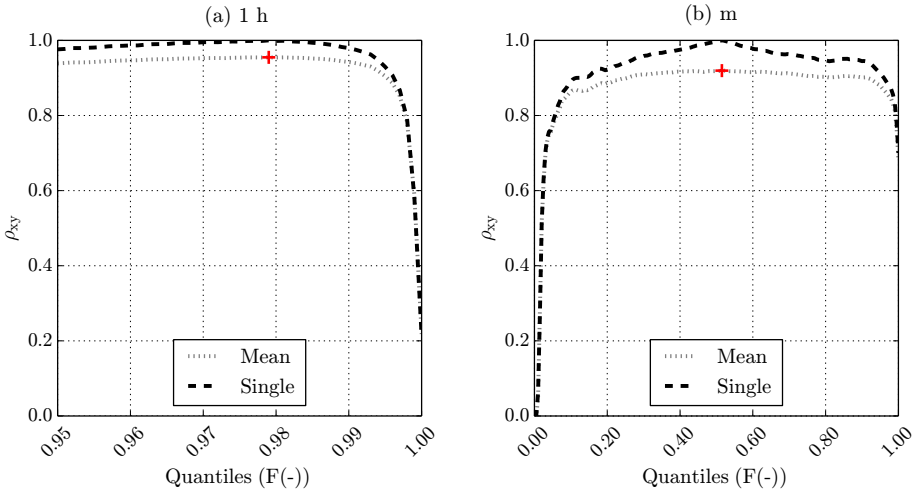

Figure 5. The mean rank correlations ρ_{xy} of the **(a)** hourly (1 h) and **(b)** monthly (m) quantile values for all gauge pairs of discrete quantiles in 0.001 (1 h) and 0.005 steps (m) ranging from Q_{th} to 1 (the gray dotted line). They are calculated to define the control quantile (Q_{c}), which exhibits the highest mean rank correlation ρ_{xy} (the red cross). The black dashed line shows the (single) rank correlations ρ_{xy} of the quantile values at Q_{c} (the red cross) with the quantile values of the remaining quantiles.

winter (from September to April). Q_{c} is mostly close to the center of the considered quantile ranges, which are also shown in Table 2. Nevertheless, the strong similarity in the winter and summer control quantiles Q_{c} is worth noting. The proposed procedure to interpolate nonparametric distribution functions using the same interpolation weights for different quantiles seems feasible, as the persistence of the order for the quantile values of the spatially distributed rain gauges is evident. Only the values of the very high and low quantiles show nonpersistent behavior. Therefore, quality measures that focus on the difference in these values will be introduced.

8 Regionalizing precipitation amount models

In the following, the regionalization of the point models in order to obtain the precipitation amount models at ungauged locations is described. The regionalization method OK is introduced first. Then, the approaches to regionalize the parametric and nonparametric distributions are explained.

As only a short overview of OK will be given, the interested reader is referred to the common geostatistical literature, like Kitanidis (1997), for further information. The empirical variogram $\gamma_e(h)$ is calculated using Eq. (19)

$$\gamma_e(h) = \frac{1}{2n(h)} \sum_{i=1}^{n(h)} (z(\boldsymbol{x}_i) - z(\boldsymbol{x}_i + h))^2, \tag{19}$$

Table 2. The control quantiles (Q_c) that exhibit the highest mean pairwise rank correlations with the other quantiles. They are shown for different temporal aggregations (agg) and separately for summer and winter. Additionally, the (center) quantile in the middle of the investigated quantile range is shown.

	Season		
Agg	Winter	Summer	Center quantile
1 h	0.977	0.979	0.975
2 h	0.963	0.967	0.965
3 h	0.959	0.966	0.96
6 h	0.949	0.953	0.95
12 h	0.924	0.922	0.93
1 d	0.835	0.865	0.86
5 d	0.615	0.575	0.645
m	0.545	0.46	0.5

where $n(h)$ is the number of gauge pairs for distance h, $\boldsymbol{x}_i$ represents the position of gauge i and $z(\boldsymbol{x}_i)$ is the variable value at gauge i. As the distances between the rainfall gauges are never a continuous set of distances, the h in Eq. (19) represents the different distance intervals. For the following applications, the width of the interval of h is 10 km and the maximum distance is 100 km. For the theoretical variogram $\gamma_t(h)$, one single model from the following four is chosen based on the least squares criterion. The s parameters represent the sills, and the r parameters represent the ranges of the variograms.

1. Gaussian model:

$$\gamma_t(h) = s_1\left(1 - e^{-\frac{h^2}{r_1^2}}\right). \tag{20}$$

2. Spherical model:

$$\gamma_t(h) = s_2\left(1.5\frac{h}{r_2} - 0.5\left(\frac{h}{r_2}\right)^3\right). \tag{21}$$

3. Exponential model:

$$\gamma_t(h) = s_3\left(1 - e^{-\frac{h}{r_3}}\right). \tag{22}$$

4. Matern model (Pardo-Iguzquiza and Chica-Olmo (2008) with K_v as the modified bessel function of the second kind):

$$\gamma_t(h) = s_4\left(1 - \frac{1}{2^{v-1}\Gamma(v)}\left(\frac{h}{r_4}\right)^v K_v\left(\frac{h}{r_4}\right)\right). \tag{23}$$

The next step within OK is solving the corresponding equation system to estimate an interpolated value at an unobserved location $\boldsymbol{x}_0$:

$$\begin{aligned} &\sum_{j=1}^{n}\phi_j\gamma_t(\boldsymbol{x}_i - \boldsymbol{x}_j) + \mu = \gamma_t(\boldsymbol{x}_i - \boldsymbol{x}_0)\ i = 1,\ldots,n,\\ &\sum_{j=1}^{n}\phi_j = 1, \end{aligned} \tag{24}$$

where n is the number of gauges included in the interpolation (10 within this work) and μ is the Lagrange multiplier.

As already outlined in the Introduction, either the parameters (Kleiber et al., 2012) or the moments (Haberlandt, 1998; Wilks, 2008) of the parametric distributions can be interpolated to regionalize the parametric models. Within this work, the moments are interpolated, when MOM is used for fitting the parametric distributions. If MLM is used, the parameters are interpolated. Since only the rainfall values above QV_{th} (see Table 1) are used, QV_{th} also needs to be interpolated within the parametric approach.

Kernel-smoothed distribution functions do not provide a parameter that can be interpolated; thus, a procedure other than that for the parametric distributions needs to be applied. When the spatial relation of the rainfall EDFs in Sect. 7 are analyzed, a persistent order of quantile values over a wide range of quantiles is observed. Therefore, the interpolation weights of the quantile values for the control quantile Q_c (see Table 2) can be applied to the remaining quantiles.

For all gauges, the quantile values QV_c of the control quantile Q_c are estimated with the inverse of the gauge-wise numerically integrated nonparametric CDF F_{np}:

$$QV_c = F_{np}^{-1}(Q_c). \tag{25}$$

With these QV_c at the observation points, the interpolation weights ϕ_j for the target locations are estimated with OK (see Eq. 24). Then, these weights are applied to the quantile values of the quantiles between Q_{th} and 1 in 0.0001 steps. Finally, the remaining quantile values are linearly interpolated to receive a continuous CDF for all target locations. In order to ensure a monotonically increasing CDF, only positive interpolation weights are allowed. This makes the use of OK problematic. It can only be used if the equation system (see Eq. 24) is solved with positive weights, which leads to additional constraints:

$$\phi_j \geq 0\, j = 1,\ldots,n. \tag{26}$$

Considering these additional constraints, the OK equation system is solved with a SCIPY implementation (Jones et al., 2001) of a FORTRAN algorithm by Lawson and Hanson (1987), which solves the Karush–Kuhn–Tucker conditions for the nonnegative least squares problem. In the following, this kriging procedure will be called positive kriging (PK). Another way to solve this extended optimization problem with an application of the Lagrange method is presented in Szidarovszky et al. (1987). The persistence of the quantile values described in Sect. 7 also implies the persistence of the quantiles. The interpolation of the quantiles for the discrete rainfall values would therefore also be an option. However, this would complicate the regionalization as not only the monotonicity needs to be preserved, but also the value range of the quantiles from 0 to 1.

9 Dependence of sub-daily on daily values

As the high-resolution rain gauge monitoring network in the study area is quite sparse and the corresponding time series are often incomplete, it would be useful to include more dense and complete secondary information in the interpolation of the sub-daily distributions. Therefore, the applicability of the daily values to improve their interpolation is investigated, as the daily monitoring network has a higher density. The simple disaggregation strategy (rescaled nearest neighbor) of Bárdossy and Pegram (2016) is applied to all days to obtain the distributions of the sub-daily resolutions at the locations of the daily gauges by allocating the sub-daily values from the closest high-resolution gauge to the daily target gauge. The procedure to incorporate the daily values in the interpolation of the sub-daily values should be the following.

1. Choose a daily target gauge and allocate the sub-daily rainfall values of the closest (concerning the horizontal distance) high-resolution gauge to it.
2. Aggregate the sub-daily values of the high-resolution gauge to the daily values $p_{\text{sub-daily}}(t)$ and calculate a scaling factor for every day t by additionally using the values of the daily target gauge $p_{\text{daily}}(t)$:

$$\text{sc}(t) = \frac{p_{\text{daily}}(t)}{p_{\text{sub-daily}}(t)}. \tag{27}$$

3. Multiply all of the sub-daily values of the nearest gauge by this scaling factor. The scaling factor changes from day to day and simply ensures that the daily sums of the disaggregated sub-daily values at the target gauge equal the daily values measured at the target.
4. Repeat steps 1 to 3 for all daily gauges.
5. Calculate the sub-daily statistic of interest from these scaled values at every daily gauge and incorporate them in the interpolation procedure.

The applicability of this procedure is tested with a cross-validation, which is described in Sect. S3. For the incorporation of the daily values within the regionalization of the parametric and nonparametric sub-daily distributions, a special regionalization technique is not needed. The rescaling method (NNS) is applied to all available daily gauges. If for a certain day no hourly values are available for the closest gauge, the next closest gauge is used for the rescaling of that day in order to increase the sub-daily sample size at the daily gauge. After obtaining the sub-daily values at the daily gauges, they are simply treated as additional control points for the regionalization.

10 Performance

This section is divided into three parts. In Sect. 10.1, the quality measures are introduced. In Sect. 10.2, the performance of the precipitation amount models for the pointwise estimations are compared for all temporal resolutions. The regionalization of the precipitation amount models is addressed in Sect. 10.3. The precipitation amount models are fitted and regionalized separately for winter (from September to April) and summer (from May to August), as the rain-producing weather processes are different in these two seasons.

10.1 Quality measures

The validation of the precipitation amount models at point locations and their regionalization is evaluated with two different quality measures. These quality measures need to be measures considering the CDF and not the PDF, as the interpolation of the nonparametric distributions only provides CDFs for ungauged locations.

The most common goodness-of-fit test to estimate the quality of fitted distributions is the Kolmogorov–Smirnov test. As distributions of precipitation amounts are positively skewed, most of the values are small or medium values, which leads to the highest gradient of the CDF for these values. Therefore, a greater difference in the corresponding CDF quantiles would be more likely and would govern the Kolmogorov–Smirnov test. However, these medium values are less important than the higher precipitation amounts for most of the precipitation model applications.

For this reason, the Cramér–von Mises criterion as a more integral measure and a Lorenz-curve-based measure, which allows for conclusions about the representation of the water volume, are used. The Cramér–von Mises criterion W^2 for single samples is (Stephens, 1974)

$$W^2 = \frac{1}{12n} \sum_{i=1}^{n} \left(\frac{2i-1}{2n} - F(x_i) \right)^2, \tag{28}$$

where $F(x_i)$ represents the theoretical distribution (nonparametric or parametric) of the observed values x_i in ascending order. For sub-monthly resolutions, the Cramér–von Mises criterion is slightly modified, as only quantiles above Q_{th} (see Table 1) are used:

$$W^2 = \frac{1}{12n} \sum_{i=1}^{n} \left(\left(\frac{2i-1}{2n} \cdot (1 - Q_{\text{th}}) + Q_{\text{th}} \right) - F(x_i) \right)^2. \tag{29}$$

As already mentioned in Sect. 7, a quality measure that describes the representation of high quantiles is needed. For Lorenz curves, high vertical differences are supposed to appear more frequently for high quantiles as the slope increases with increasing quantiles. Therefore, a measure respecting the vertical differences of the Lorenz curves is suitable. In Sect. 4, the estimation of the Lorenz curve with the observed rainfall values was described. However, the Lorenz curve $L(F(x))$ can also be estimated from the theoretical CDF $F(x)$, which is a preferable approach, as random rainfall values do not need to be generated from the CDF previous to

Table 3. The mean and median of the two quality measures W^2 and L_d for the 10 precipitation amount models over the study region for hourly values (1 h) in the winter season. The bold numbers indicate the lowest (best) value of the corresponding measure.

	W^2		L_d	
	Mean	Median	Mean	Median
P-Exp-MLM	0.009718	0.008104	0.2399	0.2004
P-Gamma-MLM	0.00263	0.002146	0.0752	0.04835
P-Mixed-Exp-MLM	0.0007967	0.0004331	0.02026	0.007648
P-Pareto-MLM	0.0006701	0.0003277	0.008036	**0.001959**
P-Weibull-MLM	0.001578	0.0012	0.03891	0.02249
P-Gamma-MOM	0.03089	0.01897	0.1656	0.04182
P-Pareto-MOM	0.001074	0.0005668	**0.004482**	0.002213
P-Weibull-MOM	0.01418	0.00827	0.08677	0.04182
NP-SRT	0.0003752	0.0001995	0.01815	0.01448
NP-SJ	**0.0003485**	**0.0001954**	0.01492	0.01156

the Lorenz curve estimation:

$$L(F(x)) = \frac{\int_0^F x(F)\mathrm{d}F}{\int_0^1 x(F)\mathrm{d}F}, \tag{30}$$

where $x(F)$ is the gauge-wise quantile function (the inverse of the CDF). The integrals of the quantile functions are estimated numerically, because the nonparametrically estimated distribution functions are not analytically invertible. The Lorenz curve criterion L_d used here is the squared difference of the observed $L(F_n(x))$ and the modeled Lorenz curve $L(F(x))$:

$$L_d = \sum_{i=1}^{n} (L(F_n(x)) - L(F(x)))^2. \tag{31}$$

The differences in the Lorenz curves are only estimated for values greater than QV_{th} (see Table 1). Within the validation of the regionalization, only the values above the highest QV_{th} among the observed and regionalized values for each gauge are evaluated, as they may differ for the different techniques.

10.2 Point models

To determine an overall performance ranking for the remaining models, the arithmetic mean and the median over the number of gauges for both measures of quality (the Cramér–von Mises criterion W^2 and the Lorenz curve criterion L_d) are first calculated for each precipitation amount model. This leads to four different measures, which are shown for hourly values in the winter season in Table 3. Note that the mean values reflect the robustness and the median values represent a good average performance of one precipitation model for the whole study region.

To combine the four statistics (the mean and median of W^2 and L_d, respectively) into one single performance measure, every value in Table 3 is then divided by the smallest (best) value (the bold numbers) of its corresponding quality measures, indicating the relative performance with respect to the best model. This leads to one number for each statistic and precipitation model starting from 1 for the best-performing model for each statistic. The bigger this number, the worse its relative performance. These four numbers are then added together, which results in a single number for each precipitation amount model to define the performance ranking for each temporal resolution. A ranking number of 4 is the lowest possible number and implies that the related model shows the best performance for all four quality measures. In Table 4, the ranking numbers for all temporal resolutions and both seasons are shown.

With the ranking numbers, the best-performing precipitation amount model is estimated for each season and temporal resolution. Among the nonparametric methods (NP), Silverman's rule of thumb (SRT) and the plug-in approach of Sheather and Jones (1991) (SJ) show very similar results. The generalized Pareto distribution with an MLM parameter estimation (Pareto-MLM) exhibits the best performance among the (P) parametric models for the hourly resolution. The mixed-exponential distribution with an MLM parameter estimation (Mixed-Exp-MLM) leads to the best results for the remaining sub-daily and daily resolutions. For temporal resolutions greater than 1 d the Weibull distribution with a MOM parameter estimation (Weibull-MOM) leads to the best results, except for the daily resolution in the winter season, where the Pareto-MOM combination is better. The best performance of the Weibull distribution for the monthly values coincides with the results of Beck (2013) for the same study region.

The performance ranking of the different methods is quite similar in winter and summer. The nonparametric methods always lead to better performances concerning the Cramér–von Mises criterion W^2. The parametric estimations lead to better results regarding the Lorenz curve criterion L_d (for details, see Tables S2 and S3). Figure 6 may provide an explanation for the differences in performance regarding these two quality measures. The graphs show the CDFs and Lorenz curves for the hourly (1 h) and 12-hourly (12 h) resolution for a chosen gauge. For the hourly resolution, the nonparametric SRT method leads to better results for both measures. An equally good performance regarding the W^2 for the parametric and nonparametric method can be observed for the 12-hourly resolution. However, the nonparametric method performs worse regarding the L_d measure, as it overestimates the water volume represented by the higher quantiles. The reason for this can already be observed in the CDF, where the nonparametric method systematically overestimates the values of the high quantiles. The parametric method can lead to overestimations and underestimations. This influences the W^2 criterion in the same way as a constant overestimation (see the squared differences in Eq. 28), but it seems to lead to better results regarding the L_d criterion.

Table 4. The performance ranking numbers of the precipitation amount models for the pointwise estimations. The underlined numbers indicate the best parametric (P) and nonparametric (NP) models. The bold numbers indicate the best overall model.

Winter season								
	1 h	2 h	3 h	6 h	12 h	1 d	5 d	m
P-Exp-MLM	225.18	145.85	129.44	69.16	37.67	41.63	14.60	742.32
P-Gamma-MLM	59.99	30.67	22.79	10.43	6.98	11.51	9.03	13.23
P-Mixed-Exp-MLM	12.93	**5.72**	**5.38**	**5.09**	**4.79**	**5.15**	15.65	742.67
P-Pareto-MLM	**6.39**	6.12	7.29	7.09	6.38	6.40	6.19	978.92
P-Weibull-MLM	30.83	14.01	9.74	5.75	4.93	7.51	6.45	24.33
P-Gamma-MOM	265.89	138.15	94.77	41.47	20.24	23.48	6.64	5.50
P-Pareto-MOM	8.11	8.8	10.23	9.25	7.96	8.08	**5.71**	51.16
P-Weibull-MOM	123.72	61.72	44.64	21.28	12.37	13.71	5.82	**5.11**
NP-SRT	13.54	22.06	35.43	42.16	36.22	31.21	17.33	12.40
NP-SJ	11.23	22.12	33.82	43.21	38.15	29.15	16.77	17.35
Summer season								
	1 h	2 h	3 h	6 h	12 h	1 d	5 d	m
P-Exp-MLM	245.24	233.50	188.82	70.63	26.14	25.83	21.67	850.52
P-Gamma-MLM	51.51	40.53	30.14	12.82	7.43	7.98	10.00	7.22
P-Mixed-Exp-MLM	10.37	**5.93**	**5.31**	**4.71**	**4.77**	**4.79**	23.10	850.52
P-Pareto-MLM	7.58	13.44	12.79	7.13	5.55	5.58	6.67	709.69
P-Weibull-MLM	21.08	13.92	10.42	6.63	5.48	6.02	6.61	25.62
P-Gamma-MOM	289.15	145.27	87.73	33.09	15.51	13.44	6.45	7.27
P-Pareto-MOM	16.48	14.46	11.55	7.28	5.99	6.08	5.82	47.81
P-Weibull-MOM	98.40	51.03	35.23	16.38	9.91	8.48	**5.46**	**5.05**
NP-SRT	**6.15**	19.05	31.54	37.41	36.15	30.76	19.00	9.27
NP-SJ	6.91	22.09	36.11	46.41	41.17	33.14	17.64	12.32

The parameter estimation through MOM in combination with the Weibull distribution performs better for the higher aggregations, which exhibit more symmetric distributions. For the daily and sub-daily aggregations, the MLM parameter estimation in combination with the mixed-exponential distribution mostly leads to the best results.

The overall performance is best with the mixed-exponential distribution for temporal resolutions between 2 hours (2 h) and 1 day (1 d) in both seasons. For the hourly distribution (1 h), the nonparametric models show the best overall performance in the summer season and the third-best performance after the generalized Pareto (Pareto-MLM and Pareto-MOM) distribution in the winter season. For the monthly resolution (m), the Weibull distribution exhibits the best overall performance in both seasons. For the 5-daily resolution, the MOM estimation provides the best result in winter (Pareto-MOM) and summer (Weibull-MOM).

10.3 Regionalization

In order to estimate the quality of the regionalized precipitation amount models, a 2-fold cross-validation (split sampling) is used. Two equally sized samples of observation points are randomly generated (Fig. 7). The simplest regionalization method is using the estimates of the nearest neighbor (NN) in the calibration set, which are therefore used as benchmarks for the quality of the regionalization procedure. Additionally, the daily rescaled nearest neighbors (NNS) are used as a benchmark. In this case, all daily gauges are used for the rescaling except for the daily observations at the locations of the respective validation sample.

Following the results of the pointwise estimation in the previous section, only the Weibull-MOM and the Mixed-Exp-MLM models among the parametric models are investigated for the regionalization, as they show good performance for differing aggregations. They are both investigated for all aggregations to test the difference for interpolated moments or parameters, except for the monthly aggregation, for which only the Weibull distribution is investigated. In order to regionalize the Weibull-MOM model, the mean and standard deviation are spatially interpolated. For the regionalization of the Mixed-Exp-MLM model, the parameters λ_1 and λ_2 are interpolated, while its parameter α is kept constant for the whole study region.

As the two nonparametric approaches SRT and SJ show very similar results during the pointwise estimation, only

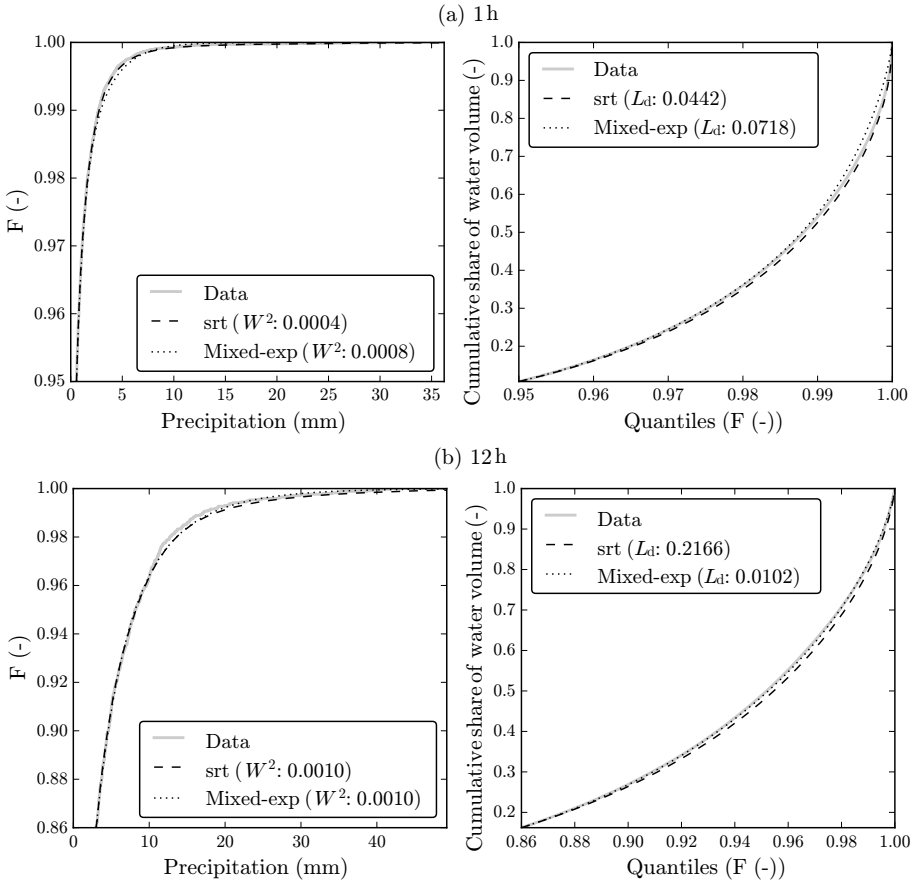

Figure 6. Empirical (data), nonparametric (SRT) and parametric (Mixed-Exp) CDF and Lorenz curve examples for the hourly (1 h, **a**) and 12-hourly (12 h, **b**) resolution of a chosen gauge. The values of the two quality measures L_d and W^2 are also indicated.

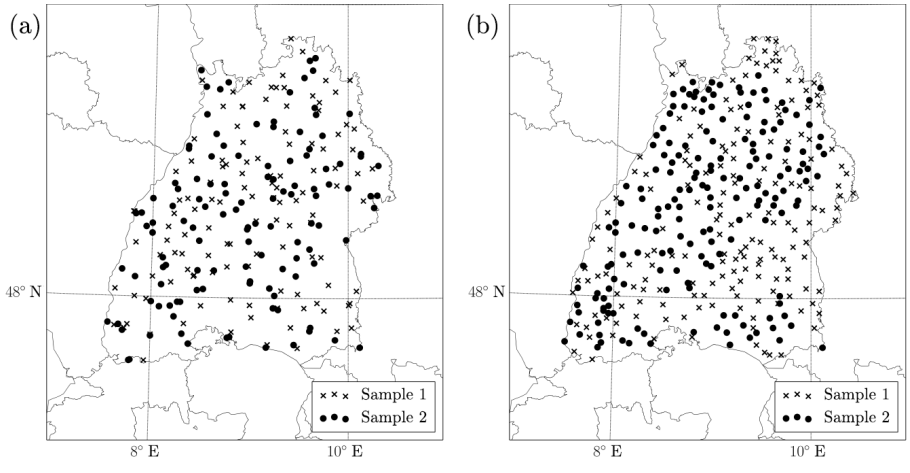

Figure 7. The locations of the two 2-fold cross-validation samples for the sub-daily **(a)** and daily gauges **(b)**.

the SRT approach is interpolated. For the regionalization of the nonparametric model, the QV_c values (see Table 2 and Eq. 25) are used to estimate the interpolation weights, which are further applied to the remaining quantiles. Following the conclusions in Sect. 9, the daily gauges can be used to set up distribution functions for the sub-daily values with a scaled nearest neighbor approach (NNS).

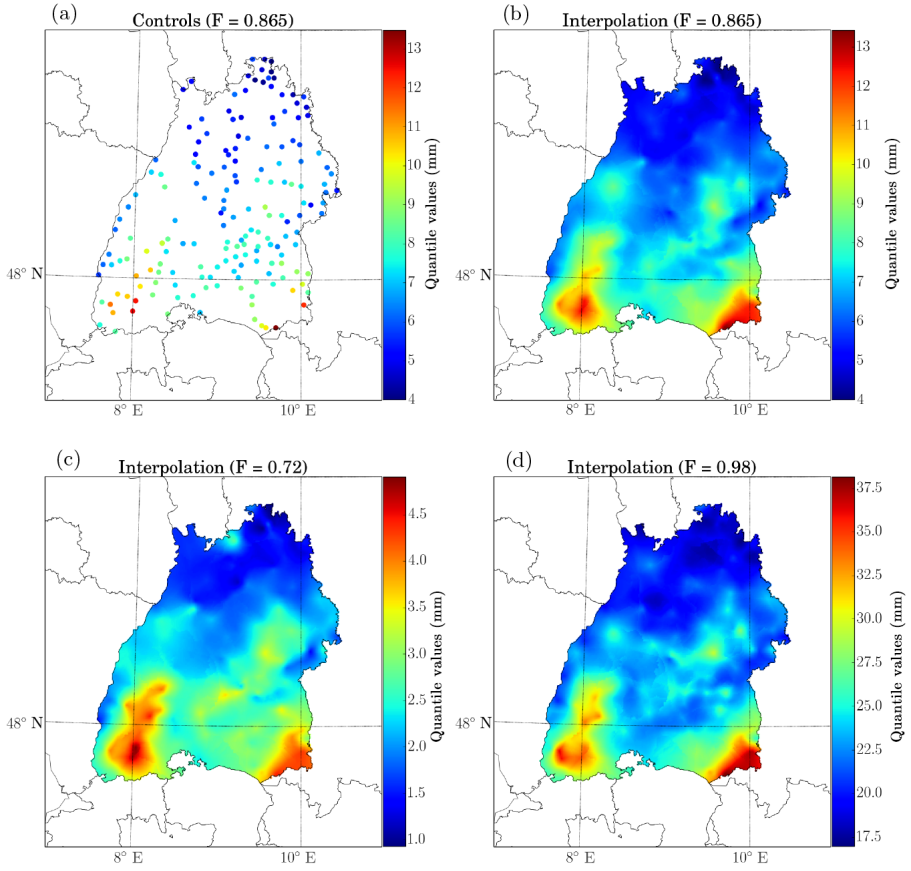

Figure 8. Illustrations for the kriging procedure of the nonparametric distributions with the daily values (1 d) in the summer season using calibration sample 1 (see Fig. 7). The **(a)** nonparametric QV_c of $Q_c = 0.865$ at the gauges, which then lead to the interpolated values **(b)** using the interpolation weights ϕ_j resulting from PK. The same interpolation weights ϕ_j are used for the remaining quantiles, for which example results are shown for the quantiles **(c)** $F = 0.72$ and **(d)** $F = 0.98$. An exponential variogram with a range of 41 km and a sill of 2.2 mm^2 is used.

10.3.1 Variogram estimation

The first step during the regionalization procedure is the estimation of the theoretical variograms. The interpolation variables of the three precipitation amount models, for which theoretical variograms need to be estimated for the two seasons and eight temporal resolutions, are as follows.

1. P-Mixed-Exp-MLM: λ_1, λ_1.
2. P-Weibull-MOM: mean, standard deviation.
3. NP-SRT: QV_c values (see Table 2 and Eq. 25).

During the estimation of the parameters of the Weibull distribution with MOM, QV_{th} is subtracted from the rainfall values prior to the estimation of the mean and the standard deviation. As the mean of these values shows lower spatial dependencies than the mean of the censored values without subtraction, QV_{th} is added to the mean values of the parameter estimation before the regionalization. After the regionalization, they are subtracted again to determine the parameters of the Weibull distribution. The variogram models are also fitted to QV_{th}, as the corresponding values serve as starting points for the parametric models at the ungauged locations. Figures S4 to S7 in the Supplement show example theoretical variograms for the different parameters for temporal resolutions of 1 and 12 h for the winter and summer seasons of calibration sample 2.

It is difficult to compare the spatial persistence of T (see Fig. 3) with the spatial persistence of the different distribution parameters (see Figs. S4 to S7), as T considers the whole distribution function and the distribution parameters only describe the properties of the distribution. However, the range of T was about 35 km, which can also be observed for some of the parameters, especially the mean of P-Weibull-MOM, the QV_c of NP-SRT and QV_{th}.

10.3.2 Precipitation amount models

The regionalization of the precipitation amount models is evaluated with the same quality measures as the pointwise es-

Table 5. The performance ranking numbers for the 2-fold cross-validation of the regionalized precipitation amount models in the winter season. The underlined numbers indicate the best parametric (P) and nonparametric (NP) models. The bold numbers indicate the best overall model for each validation sample and temporal resolution.

Calibration sample 1								
	1 h	2 h	3 h	6 h	12 h	1 d	5 d	m
OK-MOM	10.08	9.85	9.62	6.95	6.36	**4.56**	**4.37**	**4.14**
OK-MLM	7.04	7.22	7.11	10.52	6.70	7.60	6.35	–
OK-MOM DAILY	7.45	5.97	5.72	4.21	5.32	–	–	–
OK-MLM DAILY	4.46	**4.05**	**4.02**	**4.07**	**4.39**	–	–	–
PK-NP	7.18	8.21	8.94	8.98	9.21	5.56	7.24	6.94
PK-NP DAILY	**4.09**	5.74	6.00	5.68	10.09	–	–	–
NNS-MOM	7.59	6.76	6.73	5.79	7.01	–	–	–
NN-MOM	13.78	13.27	13.68	10.45	9.85	6.05	6.09	6.48
NNS-MLM	6.48	5.88	6.44	5.61	5.69	–	–	–
NN-MLM	10.04	9.81	10.39	10.19	10.51	5.41	7.40	288.07
NNS-NP	5.82	7.09	7.75	7.27	11.53	–	–	–
NN-NP	10.65	12.22	13.19	13.10	13.81	7.65	9.03	9.76
Calibration sample 2								
	1 h	2 h	3 h	6 h	12 h	1 d	5 d	m
OK-MOM	9.82	9.81	9.41	7.46	6.59	**4.00**	**4.69**	**4.14**
OK-MLM	5.19	6.19	6.87	10.29	6.73	5.45	6.85	–
OK-MOM DAILY	5.90	5.83	6.39	**4.58**	6.26	–	–	–
OK-MLM DAILY	4.33	**4.16**	**4.39**	5.62	**4.38**	–	–	–
PK-NP	5.67	8.37	10.86	11.70	9.54	6.37	9.73	7.59
PK-NP DAILY	**4.14**	6.00	7.49	8.49	11.15	–	–	–
NNS-MOM	6.24	7.06	7.09	5.51	7.42	–	–	–
NN-MOM	11.37	13.40	12.31	11.44	9.17	5.10	5.91	5.23
NNS-MLM	4.94	5.08	4.90	4.67	5.62	–	–	–
NN-MLM	7.25	9.25	9.52	9.78	8.47	4.82	6.90	283.64
NNS-NP	4.80	6.96	8.52	8.52	12.37	–	–	–
NN-NP	8.36	11.34	12.90	14.37	11.81	7.35	11.12	8.96

timation, the Cramér–von Mises criterion W^2 and the Lorenz curve criterion L_d. The investigated interpolation approaches for the parametric distributions are listed in the following.

1. OK-MOM: OK of the Weibull distribution fitted with MOM.
2. OK-MLM: OK of the mixed-exponential distribution fitted with MLM.
3. OK-MOM Daily: OK of the Weibull distribution including the scaled NNS values of the daily gauges (only for the sub-daily aggregations).
4. OK-MLM Daily: OK of the mixed-exponential distribution including the scaled NNS values of the daily gauges (only for the sub-daily aggregations).

The interpolation approaches for the nonparametric models are as follows.

1. PK-NP: PK of the nonparametric models, which are estimated using SRT.
2. PK-NP Daily: PK of the nonparametric models including the scaled NNS values of the daily gauges (only for the sub-daily aggregations).

In Fig. 8, parts of the interpolation procedure for PK-NP are shown for the daily aggregation; the nonparametric QV_c at the calibration gauges and three interpolation fields are shown.

In Tables 5 and 6, the performance ranking numbers of the regionalized precipitation amount models are summarized for the winter season and for the summer season. The differences between the two cross-validation samples are quite small, so the performances result not from the positioning of the gauges in the samples, but from the interpolation approaches. Among the parametric methods, the MOM approaches mostly perform better than the MLM approaches

Table 6. The performance ranking numbers for the 2-fold cross-validation of the regionalized precipitation amount models in the summer season. The underlined numbers indicate the best parametric (P) and nonparametric (NP) models. The bold numbers indicate the best overall model for each validation sample and temporal resolution.

Calibration sample 1								
	1 h	2 h	3 h	6 h	12 h	1 d	5 d	m
OK-MOM	34.02	13.42	10.23	7.15	**4.73**	**4.22**	**4.00**	**4.14**
OK-MLM	10.96	7.15	7.00	17.75	9.54	4.49	11.24	–
OK-MOM DAILY	22.16	13.63	10.57	5.74	9.48	–	–	–
OK-MLM DAILY	10.46	**4.19**	**4.22**	7.10	13.18	–	–	–
PK-NP	5.37	10.40	12.16	11.70	9.71	9.83	11.34	5.89
PK-NP DAILY	4.30	8.27	9.97	10.42	18.88	–	–	–
NNS-MOM	20.70	12.94	10.29	6.39	10.29	–	–	–
NN-MOM	30.16	19.43	16.53	11.26	7.72	6.18	6.41	5.55
NNS-MLM	10.37	4.36	4.48	**4.41**	7.51	–	–	–
NN-MLM	11.29	11.69	11.80	9.98	7.35	5.19	11.57	269.85
NNS-NP	**4.10**	8.79	10.26	10.72	20.24	–	–	–
NN-NP	6.26	14.98	16.41	15.95	12.41	11.59	12.70	7.84
Calibration sample 2								
	1 h	2 h	3 h	6 h	12 h	1 d	5 d	m
OK-MOM	29.60	9.95	8.78	6.61	**4.11**	**4.05**	**4.05**	**4.10**
OK-MLM	6.42	5.66	5.99	83.02	7.01	5.56	24.15	–
OK-MOM DAILY	24.89	11.54	9.23	6.02	7.11	–	–	–
OK-MLM DAILY	4.58	**4.00**	**4.00**	61.46	5.66	–	–	–
PK-NP	5.67	6.82	8.11	8.53	6.62	9.63	9.79	6.99
PK-NP DAILY	**4.27**	7.01	8.30	9.75	13.60	–	–	–
NNS-MOM	24.66	12.74	10.38	6.98	8.54	–	–	–
NN-MOM	27.71	14.10	11.90	9.10	5.81	5.81	4.82	4.90
NNS-MLM	5.53	5.09	4.91	**4.43**	6.30	–	–	–
NN-MLM	8.90	8.15	7.94	7.63	5.63	5.25	8.69	261.23
NNS-NP	5.41	7.80	9.35	10.34	14.38	–	–	–
NN-NP	9.18	10.34	11.78	9.90	7.90	10.83	10.41	8.03

for aggregations greater than or equal to 1 day during the winter season. In the summer season, the MOM approaches perform mostly worse than the MLM approaches for aggregations smaller than 6 h and vice versa for higher aggregations. Interpolating moments, therefore, seems to be more robust than interpolating parameters of the distributions as the performance ranking changed in favor of the MOM approaches compared to the pointwise results (see Table 4). Only for the more strongly skewed distributions of the smaller aggregations does the MLM approach still outperform the MOM approach.

Comparing the nonparametric interpolation approaches with the parametric interpolation approaches shows that the nonparametric approach performs best for hourly (1 h) values for both calibration samples in both seasons. This is in line with the pointwise estimations, for which the nonparametric approaches also produced very good results for the hourly resolution in both seasons.

It is obvious that using the scaled values of the daily gauges is very beneficial, as the approaches incorporating these values almost always include the best-performing method, except for the 12 h aggregation in the summer season.

As a benchmark, the interpolation results are also shown for the parametric and nonparametric estimates of the nearest neighbors (NN) and additionally using scaled daily gauges for the sub-daily aggregations (NNS). Among the benchmark methods, the NNS approaches perform better than the simpler NN approaches for the sub-daily aggregations, except for the 12-hourly (12 h) resolution in summer. Since the best interpolation approach almost always, with only three exceptions, performs better than the best nearest neighbor approach, the regionalization of the distributions seems to be worthwhile.

11 Conclusions

Comparing different modeling schemes for the precipitation amounts at point locations (see Table 4) over different temporal resolutions has revealed several findings. The nonparametric estimates only perform better for the hourly resolution in the summer season. They have problems, especially in reproducing the volume correctly, as they seem to have difficulties with high quantiles. The causes for this deficiency could be the numeric interpolation or the small number of rainfall values at high quantiles. For temporal resolutions between 2 h and 1 month, the parametric distributions outperform the nonparametric distributions for both seasons. Among the parametric methods, the MLM parameter estimation (Mixed-Exp-MLM and Pareto-MLM) performs better for the sub-daily and daily aggregations, whereas the MOM parameter estimation (Weibull-MOM and Pareto-MOM) has the advantage for higher aggregations.

The regionalization of the precipitation amount models showed (see Tables 5 and 6) that the proposed interpolation scheme for the nonparametric distributions is useful as it does not worsen its performance ranking compared to the estimation at point locations. Among the parametric methods, the interpolation of moments turned out to be more robust than the interpolation of parameters. The proposed regionalization scheme for nonparametric models could also be tested in different research fields whenever nonparametric distributions may provide good representations of pointwise models and the order of the quantiles is persistent over spatially distributed locations. Especially for applications in which multimodal distributions are common, this interpolation scheme may be of great interest because kernel density estimates, in contrast to parametric models, can easily model multimodal distributions.

As auxiliary variables, the use of daily gauges for sub-daily resolutions is very beneficial, as was suggested by our data analysis in Sect. S3 and is also proven by the evaluation of the regionalization.

In general, the regionalization of the distributions seems to be worthwhile as it nearly always performs better than the nearest neighbor (horizontal distance) approaches, which would be the simplest estimate. As lower rainfall values were excluded from this study due to their minor importance and measurement errors, the results are not directly comparable to those of most of the other publications within this research field.

The difficulty for nonparametric distributions in representing water volumes may be reduced by using the Epanechnikov kernel with finite support as proposed by Rajagopalan et al. (1997). However, the use of an Epanechnikov kernel instead of a Gaussian kernel reduces the ability to model precipitation beyond the range of historical data. Additionally, ways of incorporating elevation within the regionalization of the nonparametric distributions need to be tested. Mamalakis et al. (2017) used kriged two-component parametric distributions (a generalized Pareto distribution for higher, and an exponential distribution for lower daily precipitation amounts) for the bias correction and downscaling of rainfall resulting from a climate model. They applied a parameter estimation through probability-weighted moments, which could also be compared to the presented estimation approaches for the regionalization of distributions on varying temporal resolutions. Finally, the nonparametric interpolation approach could also be applied to parametric or empirical distributions and should be tested for various study regions.

Data availability. The sub-daily precipitation data sets used here were obtained from the LUBW during various research projects and are not available to the public as far as the authors know. Therefore, they can not be provided by the authors. The daily data set was downloaded from the WebWerdis homepage (http://www.dwd.de/DE/leistungen/webwerdis/webwerdis.html, DWD, 2017a) of the DWD, for which a personal account is required. However, to the knowledge of the authors any academic researcher can apply for a personal account, and some of the daily and sub-daily values used here also seem to be available on the homepage of the DWD Climate Data Center (http://www.dwd.de/DE/klimaumwelt/cdc/cdc_node.html, DWD, 2017b).

The Supplement related to this article is available online at doi:10.5194/hess-21-2463-2017-supplement.

Competing interests. The authors declare that they have no conflict of interest.

Acknowledgements. The work of many people developing different libraries in the PYTHON programming language (Jones et al., 2001; van der Walt et al., 2011; McKinney, 2010) made the work on the presented research much more convenient and helped a lot to illustrate (Hunter, 2007) its findings. The authors appreciate the valuable comments on an earlier draft of the manuscript by Geoffrey Pegram (University of KwaZulu-Natal, Durban, South Africa). Three anonymous reviewers helped a lot to improve the quality of the manuscript. The authors also want to thank the German Federal Ministry of Education and Research (BMBF) for funding this work through the funding measure *Smart and Multifunctional Infrastructural Systems for Sustainable Water Supply, Sanitation and Stormwater Management (INIS)*. Furthermore, the authors would like to thank the Environmental Agency of Baden-Württemberg (LUBW) and the German Meteorological Service (DWD) for the provision of rainfall data.

Edited by: D. Koutsoyiannis
Reviewed by: three anonymous referees

References

Acreman, M. C.: A simple stochastic model of hourly rainfall for Farnborough, England, Hydrolog. Sci. J., 35, 119–148, doi:10.1080/02626669009492414, 1990.

Anderson, T. W.: On the Distribution of the Two-Sample Cramer-von Mises Criterion, Ann. Math. Statist., 33, 1148–1159, doi:10.1214/aoms/1177704477, 1962.

Arns, A., Wahl, T., Dangendorf, S., Mudersbach, C., and Jensen, J.: Ermittlung regionalisierter Extremwasserstände für die Schleswig-Holsteinische Nordseeküste, Hydrologie und Wasserbewirtschaftung, HW57, doi:10.5675/HyWa_2013,6_1, http://www.hywa-online.de/ermittlung-regionalisierter-extremwasserstaende-fuer-die-schleswig-holsteinische-nordseekueste/ (last access: 28 April 2017), 2013.

Atkinson, K. E.: An Introduction to Numerical Analysis (2nd ed.), John Wiley & Sons, New York, 1989.

Bárdossy, A.: Generating precipitation time series using simulated annealing, Water Resour. Res., 34, 1737–1744, doi:10.1029/98WR00981, 1998.

Bárdossy, A. and Pegram, G. G. S.: Space-time conditional disaggregation of precipitation at high resolution via simulation, Water Resour. Res., 52, 920–937, doi:10.1002/2015WR018037, 2016.

Bárdossy, A. and Plate, E. J.: Space-time model for daily rainfall using atmospheric circulation patterns, Water Resour. Res., 28, 1247–1259, doi:10.1029/91WR02589, 1992.

Bárdossy, A., Giese, H., Haller, B., and Ruf, J.: Erzeugung synthetischer Niederschlagsreihen in hoher zeitlicher Auflösung für Baden-Württemberg, Wasserwirtschaft, 90, 548–553, 2000.

Beck, F.: Generation of spatially correlated synthetic rainfall time series in high temporal resolution: a data driven approach, PhD thesis, Universität Stuttgart, available at : http://elib.uni-stuttgart.de/opus/volltexte/2013/8216 (last access: 28 April 2017), 2013.

Bowman, A. and Azzalini, A.: Applied Smoothing Techniques for Data Analysis: The Kernel Approach with S-Plus Illustrations: The Kernel Approach with S-Plus Illustrations, OUP Oxford, 1997.

Bowman, A. W.: An Alternative Method of Cross-Validation for the Smoothing of Density Estimates, Biometrika, 71, 353–360, doi:10.1093/biomet/71.2.353, 1984.

Buishand, T. A. and Brandsma, T.: Multisite simulation of daily precipitation and temperature in the Rhine Basin by nearest-neighbor resampling, Water Resour. Res., 37, 2761–2776, doi:10.1029/2001WR000291, 2001.

Burton, A., Kilsby, C., Fowler, H., Cowpertwait, P., and O'Connell, P.: RainSim: A spatial-temporal stochastic rainfall modelling system, Environ. Modell. Softw,, 23, 1356–1369, doi:10.1016/j.envsoft.2008.04.003, 2008.

Charpentier, A. and Flachaire, E.: Log-Transform Kernel Density Estimation of Income Distribution, doi:10.2139/ssrn.2514882, 2014.

Chen, J. and Brissette, F.: Stochastic generation of daily precipitation amounts: review and evaluation of different models, Clim. Res., 59, 189–206, doi:10.3354/cr01214, 2014.

Chen, S.: Probability Density Function Estimation Using Gamma Kernels, Ann. I. Stat. Math., 52, 471–480, doi:10.1023/A:1004165218295, 2000.

Ciach, G.: Local random errors in tipping-bucket rain gauge measurements, J. Atmos. Ocean. Tech., 20, 752–759, doi:10.1175/1520-0426(2003)20<752:LREITB>2.0.CO;2, 2003.

Cohen, A. C.: Maximum Likelihood Estimation in the Weibull Distribution Based on Complete and on Censored Samples, Technometrics, 7, 579–588, doi:10.1080/00401706.1965.10490300, 1965.

Duong, T.: ks: Kernel Smoothing, available at: http://CRAN.R-project.org/package=ks (last access: 28 April 2017), r package version 1.10.0, 2015.

DWD (Deutscher Wetterdienst): WebWerdis (Web-based Weather Request and Distribution System), available at: http://www.dwd.de/DE/leistungen/webwerdis/webwerdis.html, last access: 28 April 2017a.

DWD (Deutscher Wetterdienst): CDC (Climate Data Center), available at: http://www.dwd.de/DE/klimaumwelt/cdc/cdc_node.html, last access: 28 April 2017b.

Giraldo, R., Delicado, P., and Mateu, J.: Ordinary kriging for function-valued spatial data, Environ. Ecol. Stat., 18, 411–426, doi:10.1007/s10651-010-0143-y, 2011.

Goulard, M. and Voltz, M.: Geostatistical Interpolation of Curves: A Case Study in Soil Science, 805–816, Springer, Netherlands, Dordrecht, doi:10.1007/978-94-011-1739-5_64, 1993.

Haberlandt, U.: Stochastic Rainfall Synthesis Using Regionalized Model Parameters, J. Hydrol. Eng., 3, 160–168, doi:10.1061/(ASCE)1084-0699(1998)3:3(160), 1998.

Habib, E., Krajewski, W., and Kruger, A.: Sampling errors of tipping-bucket rain gauge measurements, J. Hydrol. Eng., 6, 159–166, doi:10.1061/(ASCE)1084-0699(2001)6:2(159), 2001.

Harrold, T. I., Sharma, A., and Sheather, S. J.: A nonparametric model for stochastic generation of daily rainfall occurrence, Water Resour. Res., 39, doi:10.1029/2003WR002182, 2003.

Hosking, J. R. M. and Wallis, J. R.: Parameter and Quantile Estimation for the Generalized Pareto Distribution, Technometrics, 29, 339–349, doi:10.2307/1269343, 1987.

Hunter, J. D.: Matplotlib: A 2D Graphics Environment, Comput. Sci. Eng., 9, 90–95, doi:10.1109/MCSE.2007.55, 2007.

Jones, E., Oliphant, T., Peterson, P., et al., SciPy: Open source scientific tools for Python, available at: http://www.scipy.org/ (last access: 28 April 2017), 2001.

Jones, M. C., Marron, J. S., and Sheather, S. J.: A brief survey of bandwidth selection for density estimation, J. Am. Stat. Assoc., 91, 401–407, 1996.

Katz, R. W. and Parlange, M. B.: Generalizations of Chain-Dependent Processes: Application to Hourly Precipitation, Water Resour. Res., 31, 1331–1341, doi:10.1029/94WR03152, 1995.

Kitanidis, P. K.: Introduction to geostatistics: Application to hydrogeology, Cambridge University Press, 1997.

Kleiber, W., Katz, R. W., and Rajagopalan, B.: Daily spatiotemporal precipitation simulation using latent and transformed Gaussian processes, Water Resour. Res., 48, 1–17, doi:10.1029/2011WR011105, 2012.

Lall, U., Rajagopalan, B., and Tarboton, D. G.: A nonparametric wet/dry spell model for resampling daily precipitation, Water Resour. Res., 32, 2803–2823, doi:10.1029/96WR00565, 1996.

Landesanstalt für Umwelt, Messungen und Naturschutz Baden-Württemberg (LUBW): Klimaatlas Baden-Württemberg, available at: http://www4.lubw.baden-wuerttemberg.de/servlet/is/244295/ (last access: 28 April 2017), 2006.

Lawson, C. and Hanson, R.: Solving Least Squares Problems, SIAM, 1987.

Li, C., Singh, V. P., and Mishra, A. K.: Simulation of the entire range of daily precipitation using a hybrid probability distribution, Water Resour. Res., 48, doi:10.1029/2011WR011446, 2012.

Lorenz, M. O.: Methods of Measuring the Concentration of Wealth, Publ. Am. Stat. Assoc., 9, 209–219, doi:10.2307/2276207, 1905.

Mamalakis, A., Langousis, A., Deidda, R., and Marrocu, M.: A parametric approach for simultaneous bias correction and high-resolution downscaling of climate model rainfall, Water Resour. Res., 53, 2149–2170, doi:10.1002/2016WR019578, 2017.

McKinney, W.: Data Structures for Statistical Computing in Python, in: Proceedings of the 9th Python in Science Conference, edited by: van der Walt, S. and Millman, J., 51–56, 2010.

McMillan, H., Krueger, T., and Freer, J.: Benchmarking observational uncertainties for hydrology: rainfall, river discharge and water quality, Hydrol. Process., 26, 4078–4111, doi:10.1002/hyp.9384, 2012.

Menafoglio, A., Secchi, P., and Dalla Rosa, M.: A Universal Kriging predictor for spatially dependent functional data of a Hilbert Space, Electron. J. Statist., 7, 2209–2240, doi:10.1214/13-EJS843, 2013.

Menafoglio, A., Guadagnini, A., and Secchi, P.: Stochastic simulation of soil particle-size curves in heterogeneous aquifer systems through a Bayes space approach, Water Resour. Res., 52, 5708–5726, doi:10.1002/2015WR018369, 2016.

Nystuen, J., Proni, J., Black, P., and Wilkerson, J.: A comparison of automatic rain gauges, J. Atmos. Ocean. Tech., 13, 62–73, doi:10.1175/1520-0426(1996)013<0062:ACOARG>2.0.CO;2, 1996.

Papalexiou, S. M. and Koutsoyiannis, D.: Entropy based derivation of probability distributions: A case study to daily rainfall, Adv. Water Resour., 45, 51–57, doi:10.1016/j.advwatres.2011.11.007, 2012.

Pardo-Iguzquiza, E. and Chica-Olmo, M.: Geostatistics with the Matern semivariogram model: A library of computer programs for inference, kriging and simulation, Comput. Geosci., 34, 1073–1079, doi:10.1016/j.cageo.2007.09.020, 2008.

Peel, S. and Wilson, L. J.: Modeling the Distribution of Precipitation Forecasts from the Canadian Ensemble Prediction System Using Kernel Density Estimation, Weather Forecast., 23, 575–595, doi:10.1175/2007WAF2007023.1, 2008.

R Core Team: R: A Language and Environment for Statistical Computing, R Foundation for Statistical Computing, Vienna, Austria, availabale at: https://www.R-project.org/ (last access: 28 April 2017), 2015.

Rajagopalan, B., Lall, U., and Tarboton, D. G.: Evaluation of kernel density estimation methods for daily precipitation resampling, Journal of Stochastic Hydrology and Hydraulics, 11, 523–547, 1997.

Rider, P. R.: The Method of Moments Applied to a Mixture of Two Exponential Distributions, Ann. Math. Stat., 32, 143–147, doi:10.1214/aoms/1177705147, 1961.

Sheather, S. J.: Density Estimation, Statist. Sci., 19, 588–597, doi:10.1214/088342304000000297, 2004.

Sheather, S. J. and Jones, M. C.: A Reliable Data-Based Bandwidth Selection Method for Kernel Density Estimation, J. Roy. Stat. Soc. B, 53, 683–690, 1991.

Silverman, B. W.: Density estimation for statistics and data analysis, Chapman and Hall, London, 1. publ. edn., 1986.

Stephens, M. A.: EDF Statistics for Goodness of Fit and Some Comparisons, J. Am. Stat. Assoc., 69, 730–737, doi:10.1080/01621459.1974.10480196, 1974.

Szidarovszky, F., Baafi, E. Y., and Kim, Y. C.: Kriging without negative weights, Math. Geol., 19, 549–559, doi:10.1007/BF00896920, 1987.

van der Walt, S., Colbert, S. C., and Varoquaux, G.: The NumPy Array: A Structure for Efficient Numerical Computation, Comput. Sci. Eng., 13, 22–30, doi:10.1109/MCSE.2011.37, 2011.

Wand, M.: KernSmooth: Functions for Kernel Smoothing Supporting Wand & Jones (1995), available at: http://CRAN.R-project.org/package=KernSmooth (last access: 28 April 2017), r package version 2.23-15, 2015.

Wilks, D. S.: Multisite generalization of a daily stochastic precipitation generation model, J. Hydrol., 210, 178–191, doi:10.1016/S0022-1694(98)00186-3, 1998.

Wilks, D. S.: High-resolution spatial interpolation of weather generator parameters using local weighted regressions, Agr. Forest Meteorol., 148, 111–120, doi:10.1016/j.agrformet.2007.09.005, 2008.

Wilks, D. S.: A gridded multisite weather generator and synchronization to observed weather data, Water Resour. Res., 45, doi:10.1029/2009WR007902, 2009.

Wilks, D. S. and Wilby, R. L.: The weather generation game: a review of stochastic weather models, Prog. Phys. Geog., 23, 329–357, doi:10.1177/030913339902300302, 1999.

Woolhiser, D. A. and Pegram, G. G. S.: Maximum Likelihood Estimation of Fourier Coefficients to Describe Seasonal Variations of Parameters in Stochastic Daily Precipitation Models, J. Appl. Meteor., 18, 34–42, doi:10.1175/1520-0450(1979)018<0034:MLEOFC>2.0.CO;2, 1979.